RSC Advances

ROYAL SOCIETY OF CHEMISTRY

www.rsc.org/advances

Journal Name

ARTICLE

Near-infrared light emitting diodes using PbSe quantum dots

Received 00th January 2015,
Accepted 00th January 2015

DOI: 10.1039/x0xx00000x

www.rsc.org/

Long Yan,[a] Xinyu Shen,[a] Yu Zhang,[a,b,*] Tieqiang Zhang,[b] Xiaoyu Zhang,[a] Yi Feng,[b] Jingzhi Yin,[a] Jun Zhao,[c] and William W. Yu[a,c,d,*]

Near infrared light emitting diodes (NIR LEDs) were fabricated employing blue GaN chips as the excitation source and PbSe quantum dots as the NIR emitting materials. Quantum dots with different emitting wavelengths were selected to fabricate three NIR LEDs corresponding to two typical applications of illumination and optical communication. The variation of emission peak and full width at half-maximum of the devices were investigated under different voltage bias, and the highest external quantum efficiency of 2.52% was achieved which was comparable to those commercial InGaAsP LEDs and visible quantum dot electroluminescence LEDs.

1. Introduction

Infrared technology plays an important role in the fields of national security, geological exploration, optical fiber communication, gas sensing, illumination etc. Among them, near-infrared light emitting diodes (NIR LEDs) have received great attention because of their high power, low cost, small size, low energy consumption and long service life compared to other NIR light sources.[1-5] The manufacturing process of traditional electroluminescence NIR LEDs is complicated involving epitaxial growth, evaporation, slicing and encapsulation; the wavelength is not convenient to adjust; the production cost is still high. Therefore, it is necessary to develop a new kind of NIR LEDs.

Recently, colloidal quantum dots (QDs) have arisen for their unique properties differing greatly from the corresponding molecular and bulk materials.[6-8] Among them, colloidal lead chalcogenide QDs have been extensively investigated because they can be synthesized using simple methods for bright, narrow and adjustable NIR light emission. Thereinto, PbSe QDs have an overwhelming ability to access the strong quantum confinement, as indicated by the significant blue shift of absorption peaks with decreasing nanocrystal sizes.[9] The electron and hole are both strongly confined due to its exciton Bohr radius of 46 nm, which is approximately eight times larger than that of CdSe. PbSe QDs show extraordinary high quantum yield (up to 89%) from near- to mid-infrared wavelength range.[10-14] Therefore, PbSe QDs possess the great potential as fluorophores for NIR QD LEDs.

Incipiently, much effort were put into exploiting hybrid QD LEDs including dispersing QDs into polymer matrix and sandwiching QDs between organic carrier-transporting layers. However, the external quantum efficiency (EQE defined as the ratio of the number of photons emitted to the number of electrons injected) remained pretty low.[3,15,16] Hu *et al.* reported a ligand replacement technique of PbSe quantum dots but the EQE of this device was just 0.73%.[17] Recently, Wise group used PbS QDs to fabricate NIR LEDs employing ZnO as the carrier-transporting layer and the EQE reached 2%.[18] Bulovic group utilized PbS/CdS core/shell QDs to fabricate NIR LEDs and the use of CdS shell improved the performance compared to PbS alone. The EQE was 4.3%.[19]

Here, we utilized PbSe QDs as the luminescent material and blue GaN LED as the excitation source to create high-efficient, stable and low-cost NIR LEDs with tunable emission and this method was used to fabricate white light emitting diodes (WLEDs).[20] In a previous research, we fabricated this type of NIR LEDs to detect the gas concentration but with little performance analysis especially the efficiency of the devices.[21] As a matter of fact, the efficiency is a major parameter to evaluate a light source. Therefore, in this paper, we measured the performance parameters of three LEDs and the maximal EQE reached 2.52% which was even comparable to those commercial LEDs and visible quantum dots electroluminescence LEDs. They were also promising in the applications of optical communication and NIR lighting.

2. Experimental Section

2.1 Chemicals

[a] State Key Laboratory on Integrated Optoelectronics, and College of Electronic Science and Engineering, Jilin University, Changchun 130012, China
[b] State Key Laboratory of Superhard Materials, and College of Physics, Jilin University, Changchun 130012, China
[c] Department of Chemistry and Physics, Louisiana State University, Shreveport, LA 71115, USA
[d] College of Material Science and Engineering, Qingdao University of Science and Technology, Qingdao 266042, China
* Corresponding authors. E-mail: yuzhang@jlu.edu.cn (Y. Zhang)
wyu6000@gmail.com (W. W. Yu)

Lead (II) oxide (PbO, 99.99%), selenium powder (Se, 100 mesh, 99.99%), oleic acid (OA, 90%), 1-octadecene (ODE, 90%), tributylphosphine (TBP, 95%) and trioctylphosphine (TOP, 90%) were purchased from Alfa Aesar. Methanol, acetone, tetrachloroethylene, chloroform, hexane and toluene were obtained from Sigma-Aldrich. All chemicals were used directly without further treatment.

2.2 Synthesis of PbSe QDs

For 4.7 and 6.1 nm QDs, they were synthesized following the method previously reported by Yu et al.[9] Typically, 0.892 g PbO, 2.260 g OA and 12.85 g ODE were loaded into a three-neck flask. After 10 minutes nitrogen flow, the air in the flask was removed thoroughly. Then the temperature of the mixture was elevated to 170°C. When the yellow PbO powder was completely dissolved and the solution became colorless, 6.40 g of TOP-Se solution (containing 0.64 g Se) was quickly injected into the vigorously stirred solution. Then the temperature was adjusted to 143°C for QD growth. At a certain reaction time, 30 ml of toluene was injected into the three-neck flask swiftly and then the three-neck flask was submerged in a room-temperature water bath to completely quench the particle growth.

For the synthesis of 2.5 nm QDs, the reaction step was the same to the one above but TBP was used instead of TOP for Se.[22] 0.892 g PbO, 4.45 g OA and 9.47 ml ODE was loaded into the three-neck flask. After nitrogen flow and dissolution procedure, the temperature was kept at 90°C. 8.0 ml of TBP-Se solution (containing 0.64 g Se) was injected into the flask and the temperature was maintained at 74.3°C for 2 minutes and 20 seconds. The quenching method was the same as above.

ODE and OA have strong absorption in NIR region. Therefore, prior to the application, a series of purification operation procedures must be carried out to remove excess reaction precursors and solvents.[23] Finally, a portion of the purified PbSe QDs were redispersed in tetrachloroethylene for NIR characterizations and the others were dispersed in chloroform for LED fabrication.

2.3 LED Fabrication

Firstly, 20 mg PbSe QDs in 0.5 ml chloroform was mixed with 0.4 g UV glue. Secondly, vortex mixing and ultrasonic treatment was executed to disperse QDs into UV glue uniformly. Finally, the compound was put into a vacuum chamber to remove bubbles and chloroform thoroughly. It's worth noting that ultrasonic concussion should be executed frequently to make sure QDs homodispersed. Then PbSe QD/UV glue composites were ready for utilization. The composites were dropped on the GaN chip (2 mm × 2 mm) carefully to form a layer. After coating, the LED was loaded into UV ultra-violet ray lamp box to solidify the mixtures and the thickness of each layer was 0.3 mm. Repeated operations were carried out to make multiple layers.

2.4 Characterization of PbSe QDs and the as-prepared NIR LEDs

UV-Vis absorption spectra data were obtained by Shimadzu UV-3600 UV-visible spectrophotometer. The photoluminescent quantum yield (PLQY defined as the ratio of the number of photons emitted to the number of photons absorbed) was measured using integrating sphere technique reported by Friend and co-workers.[24] Firstly, the PbSe QDs solution was placed inside the integrating sphere (Labsphere, Inc. IS-040-SL with UV-vis-NIR reflectance coating). After being excited by monochromatic light, a fiber-coupled spectrometer equipped with a liquid-nitrogen-cooled Ge photodetector was employed to detect the emission spectra with lock-in amplification and the system response was normalized against a calibrated detector. Omni-λ300 Monochromotor/Spectrograph was utilized to get the photoluminescence spectra data including PbSe QD solutions and the as-fabricated LEDs. The optical power under different voltage and the voltage-current curve of the as-prepared LEDs were measured with Newport 1936-R power meter and Keithley 2612B SourceMeter.

3. Results and Discussion

We chose three sized PbSe QDs with diameters of 2.5, 4.7 and 6.1 nm to fabricate three LEDs. Fig. 1a shows a sequence of absorption and PL spectra of these PbSe QDs in tetrachloroethylene. The first exciton absorption peaks were 845, 1482 and 1856 nm, respectively, while the PL peaks clearly located at 946, 1545 and 1955 nm. The PL spectra had perfect Gaussian shapes and clearly indicated pure band-gap emissions.[25] They had narrow full width at half maximum (FWHM) of 142, 144 and 174 nm. The PLQYs were measured as 65%, 50% and 30% respectively. The good PLQY is the premise to achieve high EQE of the device.

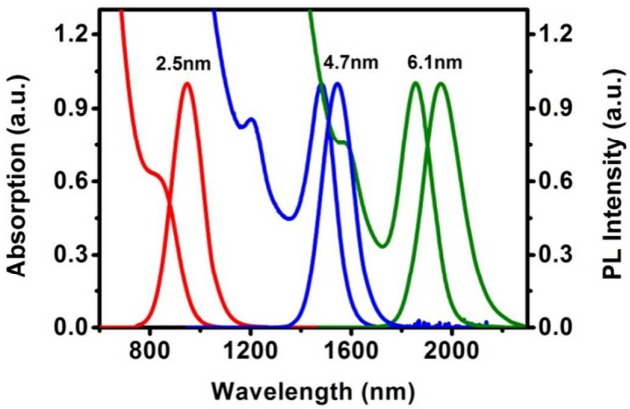

Fig. 1 The absorption and PL spectra of PbSe QDs with different sizes (corresponding to diameters of 2.5, 4.7, and 6.1 nm).

Then, the as-prepared PbSe QDs were applied as a light conversion material on a GaN LED as shown in Fig. 2. The QDs were mixed with UV glue firstly, and then we encapsulated the GaN LED with QD/UV glue composites. The UV glue was used as barrier between QDs and the chips. Therefore, this structure kept QDs away from LED chip effectively to decrease the damage caused by the thermal energy of the chip. It's worth noting that vortex mixing and ultrasonic bath should be frequently executed especially prior to application on the GaN LED chip to keep QDs homogeneously dispersed in the UV glue. We thus successfully fabricated three LEDs. The 950 nm emission NIR LED was employed as illuminating lighting source

as shown in bottom right of Fig. 2. The device photo was taken by an infrared camera when working at 3.0 V and the bright NIR light emitted by LED was clearly observed.

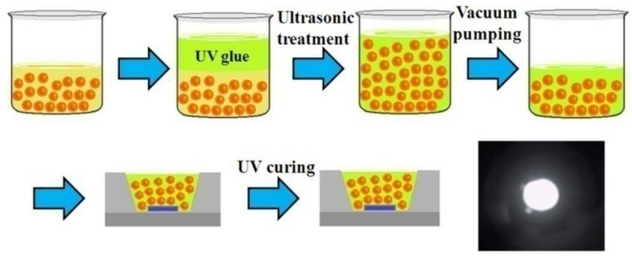

Fig. 2 The manufacturing of NIR LEDs and the working LED photo taken by a NIR-camera.

Following that, we took the 1550 nm emission LED for instance to illustrate the spectrum variation in the processing of NIR LED as shown in Fig. 3. Two emission bands of 452 and 1550 nm were contributed by the GaN blue chip and the 4.7 nm PbSe QDs, respectively. With the increase of QD/UV glue composite thickness, the emission intensity of 452 nm reduced gradually accompanied by the increase of 1550 nm emission intensity. The emission peak position of PbSe QDs remained at 1550 nm and the blue emission disappeared when the QD layer was thick enough to absorb the emission of GaN chip completely.

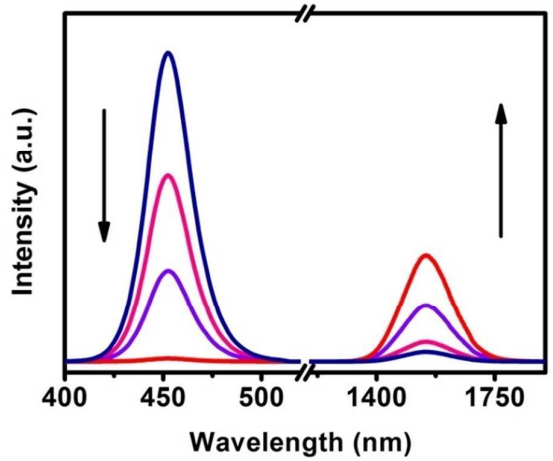

Fig. 3 The light intensity change of GaN LED emission and the PbSe QDs with QD/UV glue layer thickness.

Finally, the emission spectra of the three LEDs under different voltage are shown in Figs. 4a, b, and c, in which the emission peaks of QDs located at about 950 nm, 1550 nm and 1960 nm respectively. The intensity increased gradually along with the voltage rising. The emission of the QD LEDs had a little red-shift compared to the original solution which may be due to the QD particle aggregation in the UV glue.[26] To investigate how the UV glue affects the PbSe QDs QY, we took 2.5 nm QDs as the example which had a QY of 65% in the chloroform solution. 20 mg PbSe QDs were dissolved in 0.5 ml chloroform, then mixed with 0.4 g UV glue for device fabrication. After solidification, its QY was measured as 19.5%. We attribute the QY decline to the aggregation of the QDs in epoxy. When the concentration of PbSe QDs was fairly high, the oleic acid ligand on the surface of the QDs was not completely compatible with the epoxy polymer. Then aggregation happened.

Figs. 4d, e, and f show the FWHM and emission peak position variation of three LEDs under different voltage. The emission spectra shifted from 950 to 955.2 nm for 950 nm LED, from 1550 to 1551.5 nm for 1550 nm LED, and from 1960.5 to 1948 nm for 1960 nm LED when the voltage increased from 2.4 to 3.2 V. Red-shifts of 5.2 nm, 1.5 nm and blue-shift of 12.5 nm were observed. With the voltage going up, the temperature of the NIR LEDs would increase persistently. According to the previous reports, the FWHM increased consistently while increasing the temperature of QDs.[27-30] They changed from 142 to 159 nm (196.6 to 217.4 meV) for 950 nm LED, 145 to 159.1 nm (75.1 to 82.1 meV) for 1550 nm LED and 182 to 195 nm (56.2 to 63.5 meV) for 1960 nm LED, respectively.

This phenomenon can be attributed to the temperature variation. With the increasing voltage, the temperature of the LEDs would increase persistently. The following equation describes the temperature dependence of the excitonic peak broadening in bulk semiconductors and has been widely used for QDs.[31-33] The total line width can be described as the sum of three terms, an inhomogeneous broadening term, and two other terms representing homogeneous broadening due to acoustic and optical phonon-exciton interactions, respectively.[34]

$$\Gamma(T)=\Gamma_{inh}+\sigma T+\Gamma_{LO}\left[\exp\left(\frac{E_{LO}}{k_B T}\right)-1\right]^{-1}$$

where Γ_{inh} is the inhomogeneous line width that is temperature-independent and is due to the fluctuations in size, shape, composition, and so forth, of the nanocrystals, σ is the exciton-acoustic phonon coupling coefficient, Γ_{LO} represents the strength of exciton-LO-phonon coupling, and E_{LO} is the LO-phonon energy. Red-shift and blue-shift of LEDs were observed for the three LEDs respectively when increasing the voltage. The reason of this phenomenon is that the emission band of QDs is strongly dependent on temperature. The increasing of the temperature would lead to a simultaneous peak shift. Temperature-dependent fluorescence properties of QDs, such as CdSe and PbSe QDs, have been investigated.[25,27,35] According to the previous reports, with the increasing particle sizes of PbSe QDs, the initially positive temperature coefficient of peak energy becomes zero, and then negative.[35,36] This property is mainly derived from five factors including band gap of bulk PbSe E^0_{gap} (represents kinetic energy only), quantum confinement energy E^{conf}, electron-hole Coulomb attraction energy $E_{e\text{-}h}$, local polarization energy E^{pol}, and exciton-phonon coupling $E_{e\text{-}ph}$.

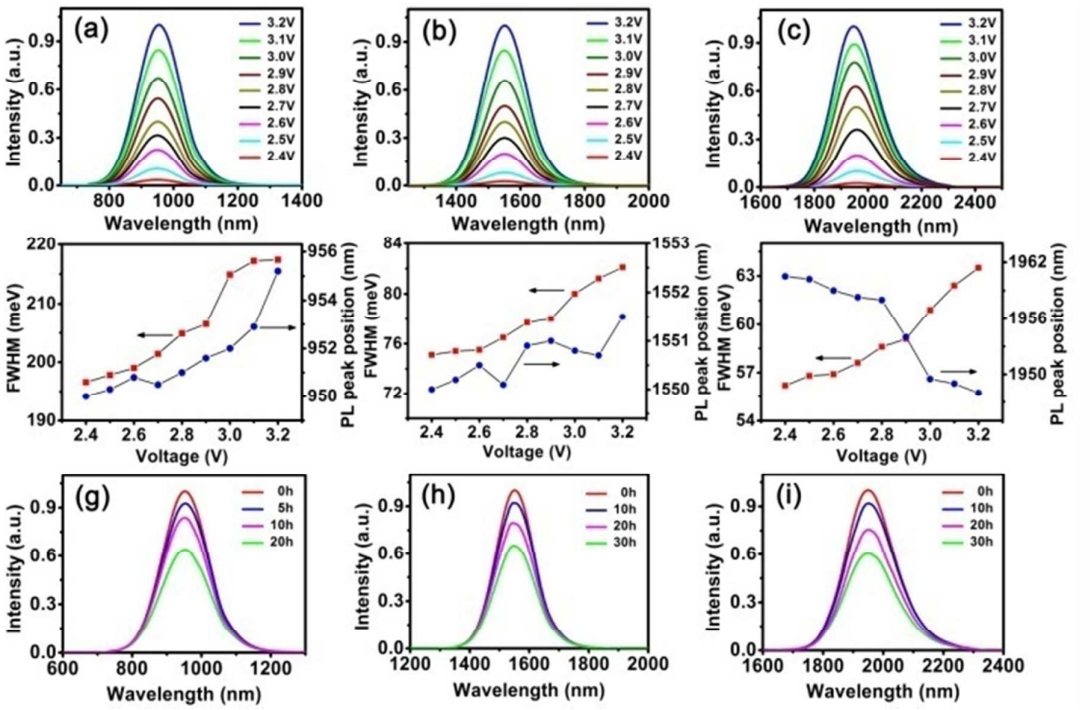

Fig. 4 The photoluminescence spectra (a) (b) (c), FWHM and emission peak variation (d) (e) (f) of 950 nm, 1550 nm, and 1960 nm LEDs under different voltage bias; the stability of (g) 950 nm (h) 1550 nm (i) 1960 nm LEDs working at 3.0V.

When temperature increases, the leading element is the lattice expansion which will lead to the increase of the bulk band gap E^0_{gap} for big size PbSe QDs. With the particle size decreases, the temperature-induced variation rate of quantum confinement energy E^{conf} becomes more influential which would compensate the variation rates of exciton-phonon coupling $E_{e\text{-}ph}$ and bulk band energy E^0_{gap}. Eventually, the temperature coefficient of PbSe QDs reduces to zero at a certain critical particle size and the band gap of PbSe QDs becomes independent on temperature. When the size decreases further, the quantum confinement-induced sized effect increases dramatically and becomes the dominant contribution. The temperature coefficient becomes negative at this moment.[37] This size-dependent temperature coefficient caused the variation of energy gap in the PbSe QDs, thus affected the emission peak positions shown in Figs 4 d, e and f.

In order to investigate the stability of the LEDs, we kept them working at 3.0V and measured their emission spectra variation. According to Figs. 4g, h, and i, the emission intensity decreased gradually when continuously working at 3.0V. After 20, 30 and 30 hours uninterrupted working, the three LEDs still maintained more than 60% of the original intensity. We attribute the emission intensity decline to two reasons: (I) the luminescent intensity of blue GaN LED decreased when working for a long time; (II) the radiant energy and thermal energy produced by GaN LED reduced the PLQY of QDs.

In order to prove our assumptions, the electroluminescent (EL) spectrum of GaN LED working for 0, 10, 20 and 30 hours were measured as shown in Fig. 5a. The emission intensity of GaN LED decreased by 13.9% after 20 hours, and 17.5% after 30 hours. The equilibrium surface temperature of GaN LED at different operating voltages was shown in Fig. 5b. When the voltage was 3.0V, the surface temperature increased to 48.3°C. Taking 950 nm LED as an example, the intensity of 950 nm LED decreased by 36% after 20 hours continuous working. The intensity decline of 13.9% was ascribed to the emission intensity dropping of GaN LED. The surface temperature of 48.3°C caused another 22.1% intensity loss.

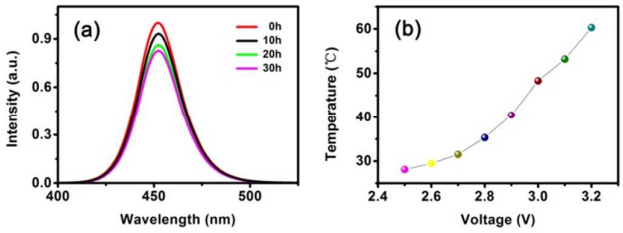

Fig. 5 The EL spectrum of GaN LED working for 0, 10, 20, 30 hours (a); the equilibrium surface temperature of GaN LED at different operating voltages (b).

To further investigate the NIR LEDs, we measured the radiation power variation as shown in Fig. 6. The radiation power gradually increased when the voltage came up. It is because the light intensity of the blue light emitted by GaN LED increased. When the voltage was raised to 3.2 V, the radiation power reached 1.09, 0.69 and 0.16 mW for the three NIR LEDs. The highest EQE of 2.52 %, 1.83 % and 0.67 % were got corresponding to 950, 1550, 1960 nm QD LEDs. The reason for the maximal conversion efficiency differences for three LEDs was the diverse PLQY for the three QDs: 65%, 50%, and 30%. Figs. 6d, e and f show the EQE variation of three LEDs with increased number of layers (the thickness of each layer was 0.3 mm). For 950 nm LED, the highest EQE was got when 8 layers of composite were applied on the GaN LED and the optimum numbers of layers were 7 and 5 for 1550 and 1960 nm LEDs, respectively. It means the optimal thickness were 2.4, 2.1 and 1.5 mm correspondingly. If the thickness was too thin, part of the blue light left out from the space between QDs. However, when the thickness was too thick, reflection and refraction would decrease the EQE. Therefore, there was the optimum thickness to obtain the highest EQE.

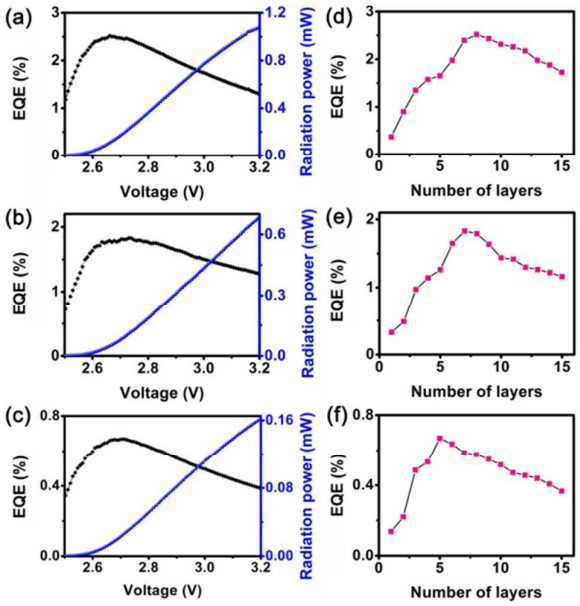

Fig. 6 The EQE and radiation power curves of (a) 950 nm (b) 1550 nm (c) 1960 nm LEDs at different voltages. The EQE variation of (d) 950 nm (e) 1550 nm (f) 1960 nm when the QD/UV glue composites were applied on the GaN LED with multiple layers.

Fig. 7 exhibits the application of three as-fabricated LEDs. In Fig. 7a, 950 nm LED was utilized as a NIR lighting source. The clear graphic proved it had great potential in the field of NIR lighting and night-vision-readable displays. 1550 nm QD LED was used in telecommunications in Fig. 7b. The light emitted by 1550 nm LED was guided into the silica optical fiber and the bright output light was observed. There was about 15% optical loss when the optical length was half meter. The output emission spectra from silica optical fiber occurred slight blue shift compared with the emission spectra in the air shown in Fig. 7c. We attributed this phenomenon to the different refractive index in the silica optical fiber for each wavelength. In conclusion, the NIR light could be transferred steadily in the silica optical fiber and the NIR LED showed great potential in the light signal transmission field as light source.

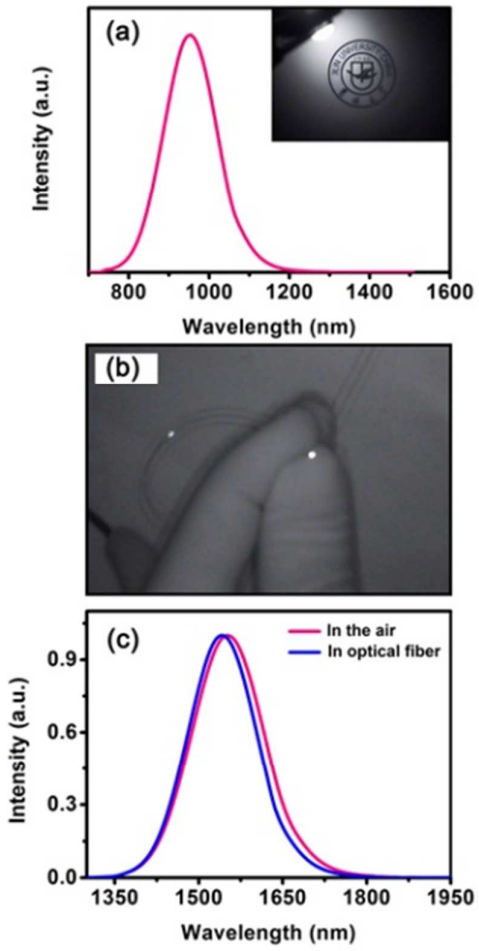

Fig. 7 The emission spectrum of (a) 950 nm LED and the inset is a photo taken by a NIR-camera in the dark employing 950 nm LED as light source; the light from 1550 nm LED was led into (b) silica optical fiber; the emission spectrum of 1550 nm LED in the air and in the (c) optical fiber.

4. Conclusions

In summary, we reported the fabrication of three QD-based NIR LEDs with different wavelengths and a detailed investigation was carried out about the properties of these NIR LEDs. Under different voltage bias, some slight changes about the emission peak position and FWHM were observed. The EQE of 2.52 %, 1.83% and 0.67% were achieved for 950, 1550 and 1960 nm QD LEDs. Finally, we showed the use of them in the field of illustration and optical communication. Combining

with the advantages of simple production process, low cost, good stability, high external quantum efficiency and the feasibility of wavelength adjustment, these QD NIR LEDs possess broad application prospects in the NIR domain. In the future work, we plan to focus on the structure optimization of these LEDs. For example, the optical coupling structures could be utilized to enhance the emission of QDs.[38]

Acknowledgements

This work was financially supported by the National Natural Science Foundation of China (61106039, 51272084, 61306078, 61225018, 61475026), the Jilin Province Key Fund (20140204079GX), the Shandong Natural Science Foundation (ZR2012FZ007), the State Key Laboratory on Integrated Optoelectronics (IOSKL2012ZZ12), NSF (1338346), NSF (2015)-LINK, and BORSF/SURE.

Notes and references

1 H. Shen, Y. Zheng, H. Wang, W. Xu, L. Qian, Y. Yang, A. Titov, J. Hyvonen and L.S. Li, *Nanotechnology*, 24 (2013) 475603.
2 T.-S. Kang, B.S. Harrison, M. Bouguettaya, T.J. Foley, J.M. Boncella, K.S. Schanze and J.R. Reynolds, *Adv. Funct. Mater.*, 13 (2003) 205-210.
3 G. Konstantatos, C. Huang, L. Levina, Z. Lu and E.H. Sargent, *Adv. Funct. Mater.*, 15 (2005) 1865-1869.
4 K.N. Bourdakos, D.M.N.M. Dissanayake, T. Lutz, S.R.P. Silva and R.J. Curry, *Appl. Phys. Lett.*, 92 (2008) 153311-153311-3.
5 K. Roy Choudhury, D.W. Song and F. So, *Org. Electron.*, 11 (2010) 23-28.
6 A.P. Alivisatos, *J. Phys. Chem. B*, 100 (1996) 13226-13239.
7 A.P. Alivisatos, *Science*, 271 (1996) 933.
8 L. Cui, X.P. He and G.R. Chen, *RSC Adv.*, 5 (2015) 26644-26653.
9 W.W. Yu, J.C. Falkner, B.S. Shih and V.L. Colvin, *Chem. Mater.*, 16 (2004) 3318-3322.
10 F.W. Wise, *Acc. Chem. Res.*, 33 (2000) 773-780.
11 H. Du, C. Chen, R. Krishnan, T.D. Krauss, J.M. Harbold, F.W. Wise, M.G. Thomas and J. Silcox, *Nano Lett.*, 2 (2002) 1321-1324.
12 C.B. Murray, S.H. Sun, W. Gaschler, H. Doyle, T.A. Betley and C.R. Kagan, *IBM J. Res. Dev.*, 45 (2001) 47-56.
13 J.M. Pietryga, R.D. Schaller, D. Werder, M.H. Stewart, V.I. Klimov and J.A. Hollingsworth, *J. Am. Chem. Soc.*, 126 (2004) 11752-11753.
14 B.L. Wehrenberg, C.J. Wang and P. Guyot-Sionnest, *J. Phys. Chem. B*, 106 (2002) 10634-10640.
15 N. Tessler, V. Medvedev, M. Kazes, S. Kan and U. Banin, *Science*, 295 (2002) 1506-1508.
16 J.S. Steckel, S. Coe-Sullivan, V. Bulović and M.G. Bawendi, *Adv. Mater.*, 15 (2003) 1862-1866.
17 W. Hu, R. Henderson, Y. Zhang, G. You, L. Wei, Y. Bai, J. Wang and J. Xu, *Nanotechnology*, 23 (2012) 375202.
18 L. Sun, J.J. Choi, D. Stachnik, A.C. Bartnik, B.-R. Hyun, G.G. Malliaras, T. Hanrath and F.W. Wise, *Nat. Nano.*, 7 (2012) 369-373.
19 G.J. Supran, K.W. Song, G.W. Hwang, R.E. Correa, J. Scherer, E.A. Dauler, Y. Shirasaki, M.G. Bawendi and V. Bulović, *Adv. Mater.*, 27 (2015) 1437-1442.
20 X. Wang, W. Li and K. Sun, *J. Mater. Chem.*, 21 (2011) 8558-8565.
21 L. Yan, Y. Zhang, T. Zhang, Y. Feng, K. Zhu, D. Wang, T. Cui, J. Yin, Y. Wang, J. Zhao and W.W. Yu, *Anal. Chem.*, 86 (2014) 11312-11318.
22 X. Zhang, Y. Zhang, L. Yan, C. Ji, H. Wu, Y. Wang, P. Wang, T. Zhang, Y. Wang, T. Cui, J. Zhao and W.W. Yu, *J. Mater. Chem. A*, 3 (2015) 8501-8507.
23 Y. Zhang, Q.Q. Dai, X.B. Li, J.Y. Liang, V.L. Colvin, Y.D. Wang and W.W. Yu, *Langmuir*, 27 (2011) 9583-9587.
24 J.C. De Mello, H.F. Wittmann and R.H. Friend, *Adv. Mater.*, 9 (1997) 230-232.
25 P. Gu, Y. Zhang, Y. Feng, T. Zhang, H. Chu, T. Cui, Y. Wang, J. Zhao and W.W. Yu, *Nanoscale*, 5 (2013) 10481-10486.
26 J. Lim, S. Jun, E. Jang, H. Baik, H. Kim and J. Cho, *Adv. Mater.*, 19 (2007) 1927-1932.
27 A. Al Salman, A. Tortschanoff, M.B. Mohamed, D. Tonti, F. van Mourik and M. Chergui, *Appl. Phys. Lett.*, 90 (2007) 093104-093106.
28 J.F. Suyver, S.F. Wuister, J.J. Kelly and A. Meijerink, *Phys. Chem. Chem. Phys.*, 2 (2000) 5445-5448.
29 S. Rudin, T.L. Reinecke and B. Segall, *Phys. Rev. B*, 42 (1990) 11218-11231.
30 W. Liu, Y. Zhang, W. Zhai, Y. Wang, T. Zhang, P. Gu, H. Chu, H. Zhang, T. Cui, Y. Wang, J. Zhao and W.W. Yu, *J. Phys. Chem. C*, 117 (2013) 19288-19294.
31 D. Valerini, A. Cretí, and M. Lomascolo, *Phys. Rev. B*, 71 (2005) 235409.
32 P. Jing, J. Zheng, M. Ikezawa, X. Liu, S. Lv, X. Kong, J. Zhao and Y. Masumoto, *J. Phys. Chem. C*, 113 (2009) 13545-13550.
33 G. Morello, M. De Giorgi, S. Kudera, L. Manna, R. Cingolani and M. Anni, *J. Phys. Chem. C*, 111 (2007) 5846-5849.
34 A. Narayanaswamy, L.F. Feiner and P.J. van der Zaag, *J. Phys. Chem. C*, 112 (2008) 6775-6780.
35 Q. Dai, Y. Zhang, Y. Wang, M.Z. Hu, B. Zou, Y. Wang and W.W. Yu, *Langmuir*, 26 (2010) 11435-11440.
36 A. Olkhovets, R.-C. Hsu, A. Lipovskii, and F. W. Wise, *Phys. Rev. Lett.*, 81 (1998) 3539-3542.
37 Y. Zhang, W. Cheng, T. Zhang, Q. Dai, T. Cui, Y. Wang, W.W. Yu, *Curr. Nanosci.*, 8 (2012) 909-913.
38 Z.-H. Chen, Y. Wang, Y. Yang, N. Qiao, Y. Wang and Z. Yu, *nanoscale*, 6 (2014) 14708-14715.

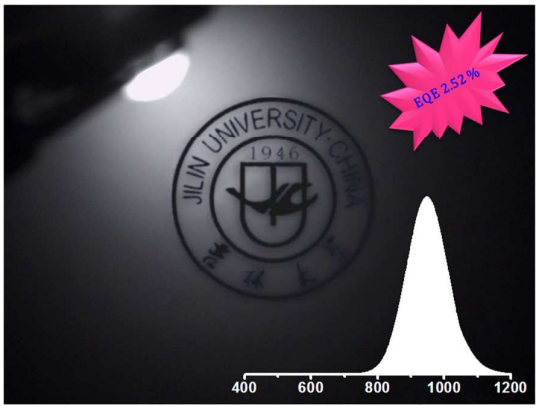

The near-infrared light-emitting diodes using PbSe quantum dots were fabticated with the highest external quantum efficiency of 2.52%, which is comparable to those commercial InGaAsP LEDs and visible quantum dot electroluminescence LEDs.